



HAL
open science

Mechanical vulnerability of beech (*Fagus sylvatica* L.) poles after thinning: Securing stem or roots is risk dependent

Jana Dlouhá, Pauline Défossez, Joel Hans DONGMO KEUMO JIAZET, François Ningre, Meriem Fournier, Thiéry Constant, Thiéry Constant

► To cite this version:

Jana Dlouhá, Pauline Défossez, Joel Hans DONGMO KEUMO JIAZET, François Ningre, Meriem Fournier, et al. Mechanical vulnerability of beech (*Fagus sylvatica* L.) poles after thinning: Securing stem or roots is risk dependent. *Forest Ecology and Management*, 2023, 552, pp.121523. 10.1016/j.foreco.2023.121523 . hal-04841046

HAL Id: hal-04841046

<https://hal.inrae.fr/hal-04841046v1>

Submitted on 16 Dec 2024

HAL is a multi-disciplinary open access archive for the deposit and dissemination of scientific research documents, whether they are published or not. The documents may come from teaching and research institutions in France or abroad, or from public or private research centers.

L'archive ouverte pluridisciplinaire **HAL**, est destinée au dépôt et à la diffusion de documents scientifiques de niveau recherche, publiés ou non, émanant des établissements d'enseignement et de recherche français ou étrangers, des laboratoires publics ou privés.



Distributed under a Creative Commons Attribution - NonCommercial - NoDerivatives 4.0 International License



Mechanical vulnerability of beech (*Fagus sylvatica* L.) poles after thinning: Securing stem or roots is risk dependent

Jana Dlouhá^{a,*}, Pauline Défossez^b, Joel Hans Dongmo Keumo Jiazet^a, François Ningre^a, Meriem Fournier^a, Thiéry Constant^a

^a Université de Lorraine, AgroParisTech, INRAE, UMR Silva, 54000 Nancy, France

^b INRAE, Bordeaux Sciences Agro, ISPA, F-33140 Villenave d'Ornon, France

ARTICLE INFO

Keywords:

Thigmomorphogenesis
Anchorage
Thinning
Guying
Stem and root growth
Beech

ABSTRACT

In this study, we analysed how the tree growth in stem and roots reacts to thinning, focusing on the consequences for mechanical stability of the root-soil plate quantified by field mechanical bending tests. In order to disentangle the role of the biomechanical control of growth (thigmomorphogenesis) from other factors, half of the studied trees were guyed to remove mechanical stimulation due to the wind of living cells. Surprisingly, our results show a decrease in the root-soil plate mechanical performances for a given stem biomass after thinning. This decrease was however explained by boosted biomass allocation to the stem at the expense of the root system. Further, relationship between the initial stiffness and the strength (overturning moment) of the root-soil plate was modified by thinning. It is suggested that at this development stage (poles), as stem break is the weakest point of tree resistance to wind loads, the biomechanical control of growth strengthens preferentially the stem and not the anchorage. Further developments should study the diversity of behaviours between development stages and between species for a unified theory on the role of the thigmomorphogenetic syndrome in tree resistance to wind risk, with synergies and trade-offs with other processes and functions.

1. Introduction

Release of competition by thinning promotes the growth of retained trees taking advantage of increased light and nutrient availability (Bréda et al., 1995; Olivar et al., 2014). However, retained trees experience also higher mechanical strains due to higher penetration of the wind into the canopy and increased sway displacements due to the loss of the stabilizing effect of collisions between adjacent trees (Rudnicki et al., 2008; Webb et al., 2013). It is well known that forest stands are much more at risk of wind hazards after a thinning (Albrecht et al., 2012; Cremer et al., 1982; Valinger and Fridman, 2011), in particular in the case of not recurrent and intensive thinning (Albrecht et al., 2015). For example Wallentin and Nilsson (2014) followed wind induced damage in recently thinned stands and observed a near-linear relationship between thinning intensity and damage with 7, 42 and 74 % of standing basal area damage in the control, normally and heavily thinned plots, respectively (8, 53 and 89 % thinning intensity). This initial increase in the mechanical vulnerability is then followed by acclimation processes leading to an increase of wind firmness. However, the transition is still poorly

understood.

The period of acclimation after thinning lasts several years and is characterised by preferential biomass allocation to the radial growth in the lower part of the stem and in structural roots and reduction of the height growth (Dongmo Keumo Jiazet et al., 2022; Mitchell, 2000; Ruel et al., 2003; Vincent et al., 2009). It has been recognized that allocation of the biomass to mechanically stimulated tissues is a result of thigmomorphogenetic response that aim at ensuring mechanical stability of trees during their life (Moulija et al., 2015; Telewski, 2006). Root growth reaction seems to be strongly affected by mechanical strains. Nicoll and Dunn (2000) reported few significant correlations between wind speed and tree ring chronologies of stem growth, but many positive correlations with the tree ring chronologies of root growth. Further, growth increase is often immediate in roots followed by one or more years delayed growth reaction in the stem (Kneeshaw et al., 2002; Urban et al., 1994; Vincent et al., 2009). However, sometimes both compartments respond with a 1-yr delay (Nicoll et al., 2019) or with no delay at all (Défossez et al., 2022).

A couple of authors tried to quantify the role of mechanical strains on

* Corresponding author.

E-mail address: jana.dlouha@inrae.fr (J. Dlouhá).

the tree growth in a forestry context coupling guying of trees with a thinning experiment, looking at the thigmomorphogenetic effect in two resource availability conditions. Defosse et al. (2022) focused on the 16 years old *P. pinaster* stem growth during three years after thinning and guying (a treatment that largely decreased strains from mechanical stimulations in growing stem tissues). They obtained similar magnitude but opposite effects of guying and thinning on the stem growth without an interaction between both factors. Nicoll et al. (2019) reported inhibitory impact of guying on the stem and root radial growth in thinned trees in a young spruce stand. Constant et al. (2018) reported that in dense beech pole stand, the mean stem growth rate at DBH of unthinned trees free to sway was multiplied by a factor 0.5 for unthinned and guyed trees, by 1.2 for thinned and guyed trees, and by 2.0 for thinned trees free to sway. Similar growth response was also observed in the roots of beech poles (Dongmo Keumo Jiazet et al., 2022), only for thinned and guyed trees the ratio yielded 1.4 instead of 1.2. Mechano-perception seems therefore to play a major role in the acclimation process of both, tree stem as well as structural roots.

As a result of mechanical acclimation, root systems of forest trees are often markedly asymmetric. Roots on the leeward side of the tree in relation to the prevailing wind direction show higher diameter growth and stronger taper than roots in other directions (Coutts et al., 2000). Specific cross-sectional shapes similar to T-beams are developed on the lee-ward side of the tree (Nicoll and Ray, 1996). Nicoll and Ray (1996) also reported that allocation to structural roots on the leeward side was strongly correlated with maximum wind speeds and this allocation appeared to be at the expense of roots further from the tree that would have had less of a structural role. Development of windward roots was correlated well with maximum gusts in the corresponding years. We can hypothesize that asymmetry of the tree growth, mechanical properties of the root-soil system may be also dependent on the prevailing wind direction.

Assessing the anchorage strength change with the tree size is not as simple as for stem resistance which is a function of the tree diameter elevated at power (Peltola, 2006). The root-soil plate is a composite structure and therefore many parameters such as the soil type and its interaction with the root system as well as the root system architecture and the root mechanical properties will contribute to determine the overall anchorage capacity of a tree and mech anical modelling provides clues to understand the role of each factor (Dupuy et al., 2007; Yang et al., 2018). In addition to these in silico approaches, field experiments have been implemented. They impose a bending force (as wind forces are bending forces) and measure the critical overturning moment which causes the failure (Gardiner et al., 2008). This critical force is obviously size-dependant (the bigger the stronger): growth increases the anchorage resistance against wind. However, because of the complexity of strength mechanisms in the root-soil plate, the effect of increased growth is not so clear. Experimental field studies observed that the overturning moment is globally a linear function of the stem biomass or $DBH^2 \cdot \text{height}$ (Lundstrom et al., 2007; Peltola et al., 2000) and the anchorage strength is characterized by the regression slope i.e. the critical force for a given stem biomass, which is the parameter used in the wind risk evaluation models to characterize the anchorage strength, removing the first order size effect (Gardiner et al., 2000). Achim et al. (2005b) reported overturning moment in a balsam fir stands thinned 9 and 14 years earlier and did not observe any increase in anchorage strength. In contrast, other studies reported higher anchorage strength in windy stands (Nicoll et al., 2008) or at the forest edge (Cucchi et al., 2004) or in widely spaced plantations (Hale et al., 2012). The latter observations were interpreted as a result of acclimation process to mechanical strains induced by wind. However, no study so far reported thigmomorphogenetic effect on the tree anchorage capacity directly.

Existing reports dealing with the tree growth and anchorage response after thinning and/or guying in the forest context focused exclusively on conifers. While growth responses are rather well documented, little is known about the acclimation of the root anchorage

strength. This study examines the growth and anchorage capacity of beech poles (pole-stage designates trees with diameter from 7.5 to 17.5 cm at DBH) after thinning and/or guying. Following hypothesis will be tested in this manuscript:

H1: beech pole anchorage capacity and growth reaction after treatment will be stronger in the direction of prevailing wind compared to across the wind.

H2: preventing the perception of mechanical strains by guying will reduce the root anchorage while increase in the mechanical strains due to thinning will increase the root anchorage. The increase should be higher than just the size effect, i.e. the increase of strength proportional to biomass growth.

H3: guying will restrict the biomass allocation to only the mechanically stimulated parts of the tree.

2. Materials and methods

2.1. Stand site and experimental design

The experimental site is located within the Haye Forest near Nancy, France (48°40'14.5"N; 6°05'10.3"E). Stand conditions are described in Bonnesoeur et al. (2016). The stand is a pure even-aged *Fagus sylvatica* L. stand resulting from natural regeneration with a Reineke's density index of 0.87 and no previous thinning. The experimental plot area is around 2 ha. Average morphological parameters of selected trees are summarized in Table 1. Four groups each consisting of ten dominant trees were selected for the study. During the winter 2014/2015 two groups were thinned removing neighbouring trees within a 4-meter radius circle centred on each target tree. Such treatment corresponds to a very strong thinning intensity. Then, half of trees (ten thinned and ten unthinned) were guyed just below their living crown. Four treatments were therefore applied: unthinned trees free to sway (uTF), unthinned and guyed trees (uTG), thinned trees free to sway (TF) and thinned and guyed trees (TG). Trees from each group were paired according to morphologic criteria (similar diameter and height). Details about selection criteria and treatments application are given in (Dongmo Keumo Jiazet et al., 2022). The site climate is a degraded oceanic type with a continental influence. Rainfall is heavy and well distributed over the year. Over the 4 years of the study, the mean annual rainfall was 700 mm and the average wind speed during the 4-year period was 3 m/s. Dominant winds came mainly from the South West quadrant.

2.2. Estimation of the stem biomass and mechanical properties of the tree stem and root-soil plate

All forty beech poles were submitted to pulling tests starting from mid-March 2019 to end of April 2019. The pulling set-up was based on Nicoll et al. (2006) and is displayed in Fig. 1. Prior to the pulling test, the tree stem was cut at 3 m height to eliminate the contribution of the crown load (Coutts, 1986). Trees were loaded using an electric winch (Winchmax, UK, maximal strength capacity 80 kN). The force applied to each sample tree was measured by a load cell (T20, AEP, Italy, maximum load 100 kN). The height of the cable attachment was low enough on the stem to induce anchorage failure without stem breakage. The latter varied from tree to tree, ranging from 1.6 m to 2.3 m. The angle of the cable θ_2 was measured when the pulling cable was stretched with a portable inclinometer. Two inclinometers (IS2BP090-I-CL; GEMAC, France) were tied to the tree to measure the root-soil system rotation θ_{1R} (at the stem base) and the total tree inclination θ_1 (close to the cable attachment point). Data from the load cell and inclinometers were recorded by a logger at a sampling rate of 20 Hz (CR1000X; Campbell Scientific Ltd., France) and uploaded to a laptop computer for processing.

The turning moment M was calculated as follows:

$$M = F_x L \cos \theta_1 + F_y L \sin \theta_1 \quad (1)$$

Table 1
Mean values of the soil humidity, the rooting depth and the mechanical characteristics of the tree root and stem resistance for each treatment. Values in brackets stand for standard error. k_{root} is the root-soil rotation stiffness, M_{root} is the overturning moment, θ_{lin} is the strain at the elastic limit, θ_{max} is the maximum strain and M_{stem} is the stem resistance.

Treatment	DBH2014 (cm)	DBH2018 (cm)	H2014 (m)	H2018 (m)	Soil water content (%)	Root depth (cm)	k_{root} (kN.m/rad)	θ_{lin} (°)	M_{root} (kN.m)	M_{stem} (kN.m)	θ_{max} (°)	Stem biomass (tkg)
TF	12.97 (0.60)	16.80 (0.57)	13.73 (0.49)	15.52 (0.52)	26.6 (2.2)	49.0 (2.5)	8196 (1133)	1.0 (0.1)	301 (34)	84.7 (9.8)	10.9 (1.2)	177.4 (15.5)
TG	12.68 (0.46)	15.05 (0.58)	14.37 (0.46)	16.19 (0.47)	25.9 (1.1)	42.7 (2.7)	6475 (1183)	0.9 (0.1)	274 (35)	58.3 (7.3)	9.6 (1.3)	170.9 (15.6)
uTF	12.60 (0.63)	14.56 (0.63)	14.02 (0.46)	15.78 (0.47)	29.2 (1.0)	41.6 (3.5)	5838 (1108)	1.2 (0.1)	270 (37)	54.9 (6.9)	10.9 (1.0)	128.4 (12.6)
uTG	12.31 (0.60)	13.28 (0.60)	14.12 (0.41)	15.96 (0.33)	26.1 (1.1)	46.9 (5.1)	4203 (835)	1.1 (0.1)	205 (35)	42.1 (5.7)	10.7 (1.2)	117.2 (10.8)

where θ_1 is the total rotation given by the deflection angle of the trunk at the cable attachment point with respect to the vertical, L is the height of the cable attachment point, $F_x = F \cos \theta_2$ and $F_y = F \sin \theta_2$ are respectively the horizontal and vertical components of the force F measured in the cable, θ_2 the angle of the cable from the horizontal (Fig. 1).

The root-soil plate initial stiffness and the elastic limit were first assessed in the direction perpendicular to the prevailing wind direction (pre-test) followed by uprooting of the tree in the prevailing wind direction (final test). The pre-test consisted in a cycling procedure with a progressive increase of the applied load for every new cycle (see Fig. 2). Once the residual root-soil plate rotation after the tree unloading was higher than 0.1° , the test was stopped. Elastic limit (θ_{lin}) was therefore computed as an interpolated value between the last elastic load step and the first post-elastic load step. Trees were then pulled until overturning thus obtaining the overturning moment (M_{root}) in the main wind direction. The root-soil plate initial stiffness (k_{root}) was computed as the slope between the turning moment and θ_{1r} in the elastic domain. To compute the root-soil plate initial stiffness in the prevailing wind direction, the elastic limit determined from the pre-test was used.

The stem resistance (M_{stem}) was computed as follows (Peltola, 2006):

$$M_{stem} = \frac{\pi * D^3 * MOR}{32}$$

where D is the tree diameter and MOR is the wood strength. As no effect of guying on the wood mechanical properties was detected, the average value of the tensile strength was used for this computation i.e. 110 MPa. Tensile tests were carried on an Instron 5969 universal testing machine equipped with 5 kN load cell using longitudinal specimens ($L \times R \times T = 15 \times 1.0 \times 0.1$ cm3) cut in the green wood. Just before the mechanical testing, rectangular heads ($L \times R \times T = 3.3 \times 3.5 \times 0.3$ cm3) were glued to each end of the specimen to enable its fixing in self-tightening grips. Strain was followed by a video extensometer AVE2 with a resolution of 0.5 μ m.

The whole stem biomass, including the topped part, was weighted using a load cell as detailed in Dongmo Keumo Jiazet et al. (2022), it is therefore a direct measure and not estimation based on partial sampling and allometric relationships that might be affected by treatments on the studied trees.

2.3. Soil and root characterization

The study area is part of the larger area known as the Lorraine plateau (6.1°E, 48.7°N). Three rectangular soil pits (1 m \times 0.4 m) were manually dug in the stand down to the calcareous bedrock horizon. The soil is a rendosol where rooting is constrained by a stony layer with 70–90 % of stones at 34.3 ± 7.7 cm depth. Above this stony layer two clay-silt horizons may be distinguished above and below 10 ± 1.2 cm depth, containing together all roots with diameter > 2 mm. Limestone bedrock is situated at 79.5 ± 14.8 cm. Once the root-soil plate was extracted, the maximal rooting depth was measured as well as the depth of the two visible horizons. A soil sample of 0.25 l (cylinder of 5 cm depth and 8 cm of diameter) was taken in the middle of each horizon, placed in an aluminium box sealed with plastic for subsequent determination of gravimetric soil water content. Gravimetric soil water content was determined by comparing fresh and dry weights (24 h at 105.0 °C) of the soil sample from each horizon. Weighted gravimetric soil water content was then computed as a weighted mean taking into account the depth of each soil horizon.

2.4. Root growth ring measurements

Extracted root systems were first cleaned in the forest with an air compressor (LOXAM 2000 l/min, 7 bar, blowing lance LACME 40 m³/h 670 l/min), before finer cleaning using a high-pressure water in the laboratory. Four of the largest structural roots were cut at 0.25 m

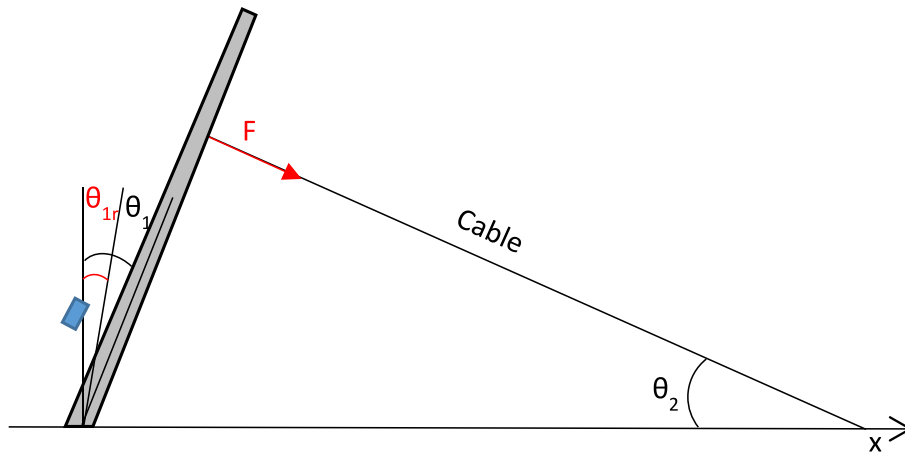


Fig. 1. Set-up of the pulling test. θ_{1r} is the root-soil plate rotation, θ_1 is the trunk deflection angle and θ_2 is the cable inclination. F is the pulling force. Blue boxes represent location of inclinometers.

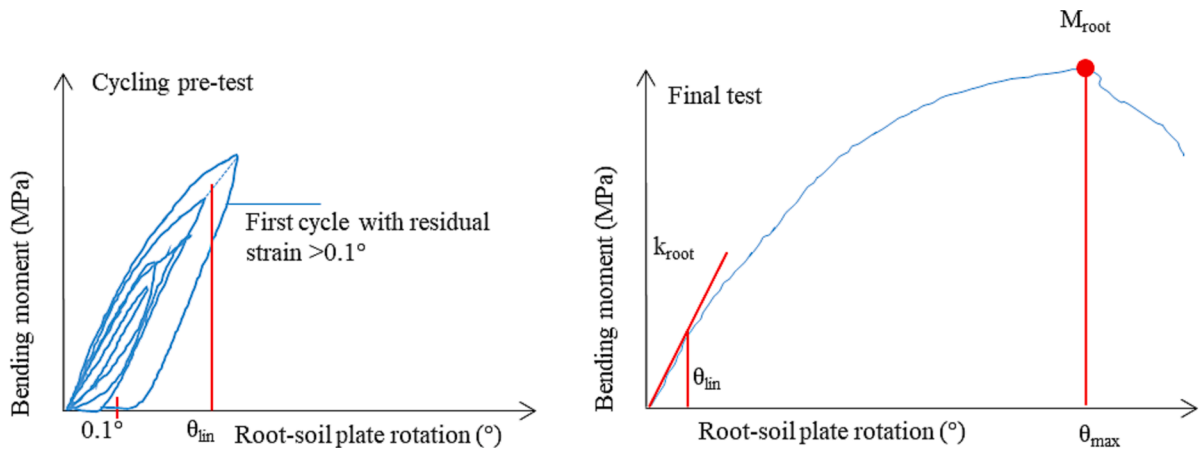


Fig. 2. Estimation of mechanical performances of the root-soil plate from the experimental curve. θ_{lin} stands for the elastic strain limit, k_{root} stands for the initial root-soil plate elasticity and M_{root} stands for the overturning moment. Figures are not proportional, the pre-test figure is magnified in order to make the elastic limit visible.

horizontal distance from the stump centre. The selected roots were distributed around the tree to represent different quadrants in respect to the wind direction, leeward quadrant (North-East) and windward (South-West) quadrant were designated by 1 and 2 respectively and quadrants perpendicular to the prevailing wind direction were designated by 3 and 4. The biggest roots in each quadrant were selected and a 2-cm thick cross-sectional root sample was scanned with an optical scanner at 600 dpi resolution and growth rings were measured using Image-J software (Schneider et al., 2012). The upper side of each root was marked and the root growth ring widths were measured only in the maximal growth direction from the upper-side outer ring to the biological centre of the root. For the sake of simplicity, we will not talk about average maximal root growth ring indicator but about mean root growth ring. It happened that some quadrants could not be sampled because roots were broken. Altogether, 122 root samples equally distributed among treatments were measured. A stem disk was also collected at breast height to compare the growth response at the stem and root level. The methodology to analyse stem and root samples is further detailed in Dongmo Keumo Jiazet et al. (2022).

2.5. Statistical analysis

Statistical analyses were performed using R-software (R Core Team, 2020). We first used ANOVA on lm model to check that there were no difference in the soil water content during pulling tests as well as in the

rooting depth of the tree groups (corresponding to each treatment) according to the following model:

$$\text{anova}(\text{lm}(\text{rooting_depth}/\text{water content} \sim \text{treatment})).$$

In further analysis, we considered the factorial design of our experiment testing the two main effects, thinning and guying, together with their interaction.

First, linear mixed effects model (nlme package) with pairing as a random effect was used to assess the effects of thinning, guying and their interaction on mean values of the root system properties displayed in Table 2:

Table 2

P-values of the main effects and their interaction (guying and thinning) of linear mixed effect models (model 1). k_{root} is the root-soil rotation stiffness, M_{root} is the overturning moment, θ_{lin} is the strain at elastic limit and M_{stem} is the stem resistance. Figures in bold designate significance at the 5% level.

	Effects		
	Thinning	Guying	Thinning × Guying
k_{root}	0.0029	0.0184	0.86
θ_{lin}	0.0532	0.4773	0.94
M_{root}	0.047	0.0107	0.18
θ_{max}	0.3028	0.1834	0.37
M_{stem}	0.0002	0.0001	0.39
Stem biomass	<0.001	0.0620	0.56

Table 3

P-values (model 2) of main effects and their interaction on relationships between the root system mechanical properties and the stem biomass or between different root and stem mechanical properties. figures in bold designate significance at the 5% level.

	Effects on intercept			Effects on slope		
	Thinning	Guying	Thinning × Guying	Thinning	Guying	Thinning × Guying
$k_{root} \sim$ Stem biomass	0.04	0.09	0.95	0.48	0.70	0.64
$M_{root} \sim$ Stem biomass	0.0003	0.18	0.95	0.04	0.58	0.77
$M_{root} \sim k_{root}$	0.03	0.52	0.80	0.015	0.32	0.30
$M_{root} \sim M_{stem}$	0.03	0.28	0.54	0.006	0.40	0.69
$k_{root} \sim k_{root90}$	0.30	0.99	0.69	0.31	0.44	0.69
Stem biomass $\sim D^3$	0.52	0.0199	0.16	0.84	0.49	0.79

Table 4

P-values (model 3) for main effects and their interaction on the relationship between the mean growth ring in the stem and in roots. figures in bold designate significance at the 5% level.

Effect	p-value
(Intercept)	<0.0001
Guying	<0.0001
Thinning	<0.0001
Period	0.0001
Root_ring	<0.0001
Guying × Period	0.0043
Thinning × Period	0.0003
Guying × Root_ring	0.0130
Thinning × Root_ring	0.6446
Period × Root_ring	0.1070

Model 1: $\text{lme}(y \sim \text{Thinning} * \text{Guying}, \text{random} = \sim 1 | \text{Paired_id}, \text{method} = \text{"REML"})$.

Effects of thinning, guying, and their interaction on relationships between the root system mechanical properties and their predictor (stem biomass) or between mechanical properties themselves, were assessed using gls models because their AIC were systematically lower than for mixed effects models (Table 3). Models were formulated as follows:

Model 2: $\text{gls}(y \sim \text{Thinning} * \text{Guying} + (\text{Thinning} * \text{Guying}) * x, \text{method} = \text{"ML"})$.

This model was also used to examine the anisotropy of the root-soil plate stiffness and the relationship between the stem biomass and DBH^3 . Relationship between the root and the stem growth increments before and after treatments were assessed using linear mixed effects models with tree number as a random effect to take into account repeated measurements, introducing of pairing as a random effect did not improve the model. The best fitting model (lowest AIC) was of the following form (results are summarized in Table 4):

Model 3: $\text{lme}(\text{Stem mean ring width} \sim (\text{Thinning} + \text{Guying}) * \text{Period} + (\text{Thinning} + \text{Guying} + \text{Period}) * \text{Root mean ring width}, \text{random} = \sim 1 | \text{TreeNb}, \text{method} = \text{"REML"})$.

We assessed the normality of the data distribution with Q-Q plots, and homoscedasticity with standardized residuals against plotted fitted values and when necessary with Levene tests (package car (Fox and Weisberg, 2019)). Weighted regressions, as a function of thinning, were used for M_{root} against M_{stem} and M_{root} against k_{root} predictions. The significance level of 5 % was used in all analysis.

3. Results

Table 1 summarizes mean values of the morphological parameters, the test conditions and the mechanical parameters for each treatment. We can see that there was no significant difference in the soil water content between the four groups and the rooting depth was also the same. Considering the effect of thinning, guying and their interaction on the root-soil mechanical properties, models revealed that interaction

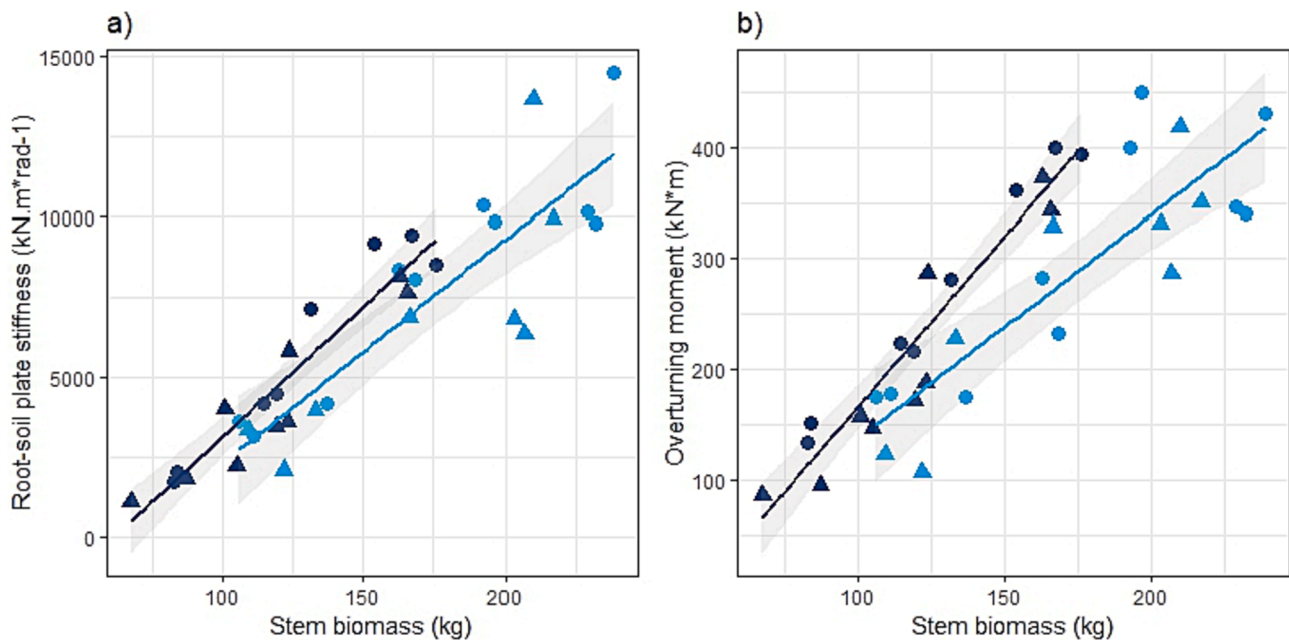


Fig. 3. A) Relationship between the root-soil plate stiffness and the stem biomass. b) Relationship between the overturning moment and stem biomass. Dark blue regression lines and points represent unthinned trees. light blue regression lines and points represent thinned trees. Triangles stand for guyed trees and circles for trees free to sway.

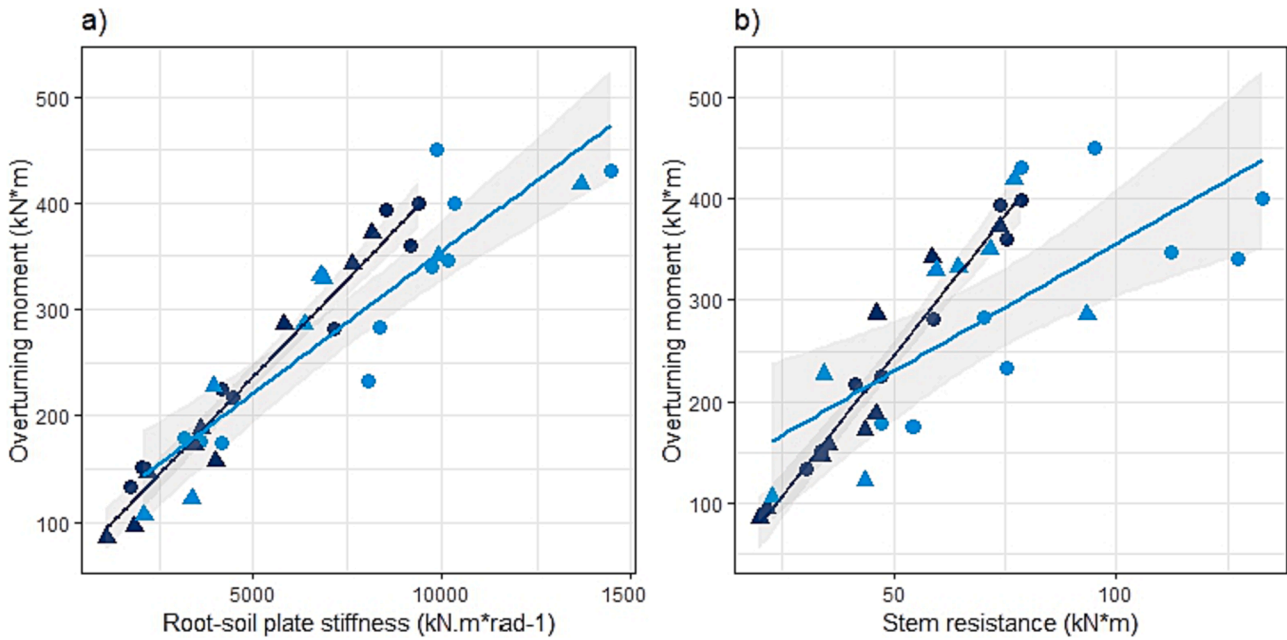


Fig. 4. A) Relationship between the overturning moment and the root-soil plate initial stiffness. b) Relationship between the overturning moment and the stem resistance. Dark blue lines and points represent unthinned trees. light blue lines and points represent thinned trees. Triangles stand for guyyed trees and circles for trees free to sway. Solid lines represent regression line for trees free to sway.

factor (thinning × guyying) was not significant (Table 2) while thinning and guyying effects were significant for all properties tested except for the strain at elastic limit and maximal strain, with very high significance especially for the stem resistance. Thinning strongly affected the stem biomass while guyying effect was not detected. Observed elastic limit of the root-soil plate rotation θ_{lin} did not differ with the treatment but was higher than the threshold typically used for the non-destructive evaluation of the tree failure (Brudi and Wassenaer, 2001; Detter et al., 2023) or identified in sub-alpine spruce (Jonsson et al., 2006) which was 0.25° and 0.5° respectively. However this limit was close to the elastic limit

experienced by Eucalyptus trees in natural conditions (James et al., 2013) i.e. 0.88–0.9°.

Fig. 3 shows the relationship between the root-soil plate stiffness and the overturning moment against the tree stem biomass. We can see that thinned trees display surprisingly lower root system anchorage properties for a given stem biomass compared to unthinned trees. In the root-soil plate stiffness case, the regression line for thinned trees is shifted downwards while for the overturning moment, thinning affects the intercept as well as the slope of the relationship against the stem biomass (see Table 3). For example a tree with 150 kg stem biomass from the

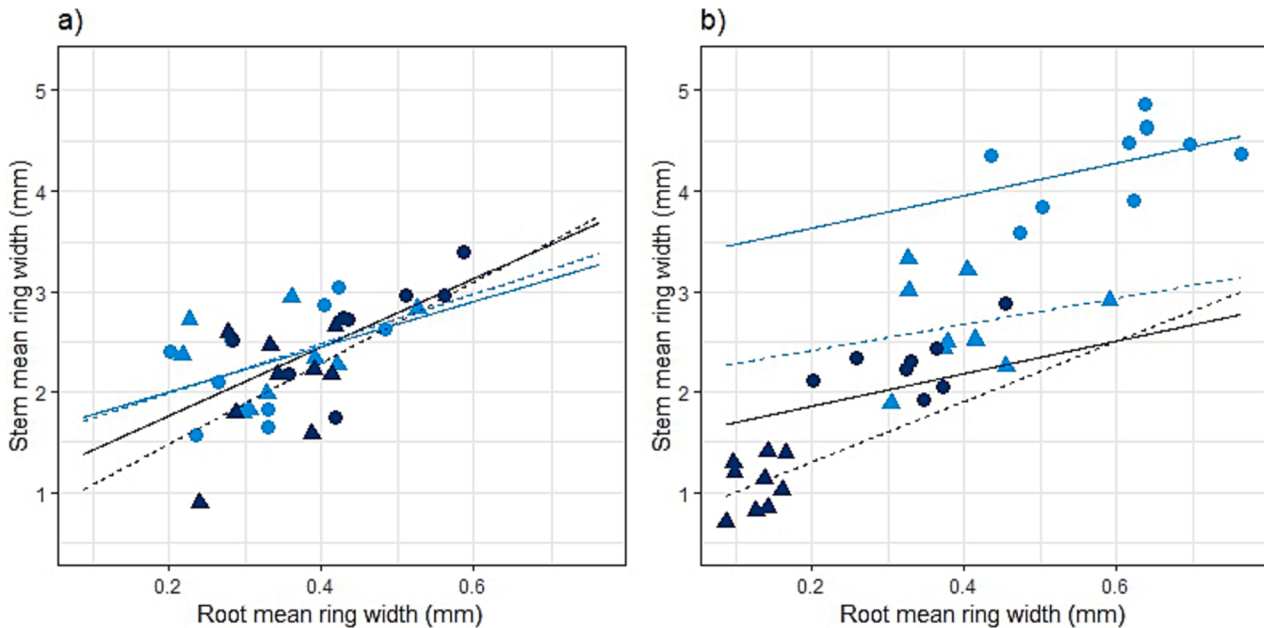


Fig. 5. Relationship between the stem mean ring width and the root mean ring width before (a) and after treatments (b). Each point represents the mean growth ring width over a four years period. Light blue regression lines and points represent thinned trees, dark blue regression lines and point represent unthinned trees. Triangles stand for guyyed trees and circles for trees free to sway. Solid lines represent regression line for trees free to sway and dotted lines represent regression lines for guyyed trees.

Table 5

Mean values of the root ring width for a given treatment, time period and direction. Direction 1 = NorthEast, leeward side, direction 2 = SouthWest, direction 3 = SouthEast, direction 4 = NorthWest.

Treatment	Direction	Before		After	
		Root growth (mm)	Standard error (mm)	Root growth (mm)	Standard error (mm)
uTF	1	0.53	0.04	0.38	0.03
uTF	2	0.39	0.04	0.30	0.03
uTF	3	0.45	0.03	0.33	0.02
uTF	4	0.42	0.04	0.31	0.03
uTG	1	0.34	0.03	0.12	0.01
uTG	2	0.35	0.03	0.12	0.01
uTG	3	0.34	0.05	0.18	0.03
uTG	4	0.41	0.04	0.17	0.02
TF	1	0.36	0.03	0.69	0.03
TF	2	0.31	0.03	0.53	0.04
TF	3	0.35	0.04	0.60	0.03
TF	4	0.31	0.03	0.54	0.03
TG	1	0.34	0.02	0.45	0.03
TG	2	0.30	0.03	0.35	0.03
TG	3	0.37	0.03	0.40	0.03
TG	4	0.34	0.04	0.33	0.02

unthinned plot will achieve an overturning moment of 336kN*m/rad against 232kN*m for a 150 kg tree from the thinned plot which is a decrease of 44.8 %.

Fig. 4a shows that after thinning, the slope of the regression line between the overturning moment and the root-soil plate elasticity is lower. Considering the balance between the overturning moment and the stem resistance (Fig. 4b), we can clearly see that thinned trees invest more in their stem resistance compared to the anchorage strength. We can also notice the higher dispersion of points corresponding to thinned trees. Indeed, the slope (estimate and standard error) of the regression line is very close in unthinned trees (5.77 ± 0.58 and 5.38 ± 0.55 for uTF and uTG respectively) while more distinct in unthinned trees even if the difference is not significant (2.52 ± 0.85 and 3.60 ± 1.26 for TF and TG, respectively).

After the analysis of the root and stem mechanical properties, we measured the biomass allocation between the tree compartments (stem and structural roots) before and after the treatments. We looked first at the mean root and stem growth ring over the period of four years. Fig. 5a shows that there is no significant difference between the four groups before treatments. Table 4 further shows that main effects (guying, thinning and period) are concentrated on the intercept which is confirmed in the Fig. 5b where regression lines for each treatment are horizontally shifted. When comparing selected contrasts, TG and uTF trees do not show any change in the biomass allocation between the tree compartments before and after the treatments (p-values 0.61 and 1 respectively) while TF clearly allocate more biomass to the stem compared to structural roots after thinning (p-value 0.0019).

We further looked at the directional allocation of the biomass in roots in function of the main wind direction. Mean root ring and its standard error for a given treatment, period and direction is summarized in Table 5. Results of statistical tests revealed no effect of the direction before treatments ($p = 0.13$) while after treatments, direction was statistically significant ($p = 0.00$). Paired tests showed that direction 1 (leeward side) was significantly different from direction 2 and 4 (p-values 0.0002 and 0.0008 respectively). However, no difference with direction 3 was detected which has no biomechanical meaning (we would expect more allocation along the dominant wind axis *i.e.* direction 1&2). Furthermore, the interaction term between the treatment and direction is not significant ($p = 0.14$). Considering the anisotropy of the root-soil plate initial stiffness with respect to the pulling direction, no effect of guying or thinning was detected (Table 3). When we looked at confidence interval of the regression parameters, the slope was not significantly different from unity ($p = 0.49$) and the intercept not

significantly different from zero ($p = 0.096$).

4. Discussion

4.1. No directional anisotropy was detected in the growth of structural roots and the initial root-soil plate stiffness

In windy locations, root systems exhibit anisotropic growth with more structural root mass on the leeward side than the windward side of the tree relative to the prevailing wind direction (Nicoll and Ray, 1996). However data about the directional dependence of mechanical performances of the root-soil plate are lacking. In this study, we measured the initial stiffness of the root-soil plate in two directions: the prevailing wind direction and perpendicular to it. No directional difference was observed in the initial stiffness of the root-soil plate. However, the latter may reflect more the development of fine roots and coherence of the root system with the neighbouring soil than the thickening of structural roots that is involved in later phases of mechanical loading even if both parameters are in general well related (Jonsson et al., 2006). We therefore looked also at the growth in structural roots in function of the direction of the wind loading. However again, no directional preference for biomass allocation was detected along the wind direction axis. This result is in agreement with the fact that even if the wind loading at our site is anisotropic with a defined prevailing wind direction, anisotropy of the mechanical strain perceived at the periphery of the stem is much lower and likely not anisotropic enough to trigger anisotropic distribution of the growth around the stem periphery (Dongmo Keumo Jiazet, 2022).

4.2. Thinning surprisingly decreased the mechanical properties of the root-soil plate for a given stem biomass

It is widely accepted that thinning reduces the long-term risk of wind damage. However, immediately after the thinning trees are on the contrary more prone to fail mechanically (Wallentin and Nilsson, 2014). This initial mechanical vulnerability after thinning is in general attributed to increased wind penetration into the canopy and lack of neighbours, when the intrinsic resistance of trees is not yet acclimated to new conditions. Thigmomorphogenesis would be expected to increase biomass allocation to the tree parts experiencing high strains, typically the bottom part of the stem and structural roots in order to reduce the mechanical risk, increasing the mechanical strength of the anchorage during the few years of the transition period after thinning. Indeed, a couple of studies report increase in the root growth after thinning and that is hindered by guying (Dongmo Keumo Jiazet et al., 2022; Nicoll et al., 2019). However the relation between the root growth and the change in root-soil plate mechanical properties is not straightforward. Considering the root-soil plate mechanical properties, to our knowledge only the effect of thinning has been reported and no study exists on the root-soil plate mechanical properties of guyed trees. Achim et al. (2005a) studied the effect of thinning on the overturning moment of balsam fir 9 and 14 years after thinning and did not show any effect of thinning on the relationship between the overturning moment and stem biomass. But 9 and a fortiori 14 years after the thinning, the transition period might be over, thus only confirming the finding that different spacing does not affect the overturning moment-stem biomass relationship as established by Nicoll et al. (2009) and confirmed recently for example by Kamimura et al. (2017).

Surprisingly, our study shows lower mechanical properties of the root-soil plate for a given stem biomass after thinning for the elastic part of the response as well as for the final overturning moment (Fig. 3). Such finding might at the first sight contradict the capacity of the thigmomorphogenesis to ensure the mechanical security of the tree. It was also found that the relationship between the initial stiffness of the root-soil plate increased more than the overturning moment after the thinning (Fig. 4). As mentioned by Yang et al. (2020), the elastic stiffness of the

root-soil plate is crucial for the mechanical stability of the tree due to the fatigue in roots system occurring during successive wind gusts and therefore it should be reinforced in priority. Whereas removing the perception of the mechanical signal has changed cambial growth in stems and roots (Dongmo Keumo Jiazet, 2022), no effects were detected on the scaling of mechanical properties of the root-soil plate with the stem biomass. As the mechanical behaviour of the root-soil plate is not, on the contrary to the stem, mainly influenced by the radial growth of one single beam, it will be interesting to study more accurately changes of root architecture after thinning and trade-offs between several needs and constraints. Indeed, the biomass of fine roots is known to significantly increase after thinning (López et al., 2003) and change in the fine root biomass production is found to be more sensitive to thinning than in thicker structural roots (Pang et al., 2022). It might be very interesting to check the proportions of fine roots in further studies and study their role in mechanical properties. Then, for further ecological studies, we suggest studying to what extent the initial stiffness of the root-soil plate might be used as a mechanical but also hydraulic trait.

The main clue to enlighten the unexpected decrease of the root-soil plate mechanical properties with thinning is given in Fig. 4b showing the relationship between the overturning moment and the stem resistance. We can see that the slope of the regression is high in unthinned trees (5.38 for uTF, 5.77 for uTG) and is reduced in TG (3.60) and in particular in TF trees (slope = 2.52). Forest managers know (personal communication, François Ningre) that for this size of beech trees, the main mechanical damage observed at this developmental stage is the stem breakage while uprooting is not often observed. This observation is also in line with the model prediction of windthrow probability that is relatively low in small beech trees (around 0.2 for a 16 m high beech tree based on Bonnesoeur et al. (2013)). The balance between the windthrow and stem breakage risk is among other parameters (rooting depth, soil properties etc.) species and size dependent. Beech is a rather well rooted species with a tendency to break rather than uproot in young stages compared for example to spruce (Stokes, 2000) whereas on very thin

soils of Lorraine plateau, beech was described as sensitive species to windthrow with increasing size (Bonnesoeur et al. 2013). This change in mechanical weak point location and failure modes with tree age and size must be considered when studying changes in biomass allocation between compartments. For example Urban (1994) reports a 3 to 9 years delay of the growth response in the stem compared to roots reacting immediately after a road clearing in a 120 years old white spruce stand where uprooting might be the main mechanical threat while in younger stands with smaller trees, such delay is in general not observed (Defosse et al., 2022; Nicoll et al., 2019). Higher sensitivity to wind signals of roots when compared to stem was also reported on rather big trees (46 years old spruce (Nicoll and Dunn, 2000)) indicating that tree size may play an important role in the reactivity of different tree compartments to wind loading. This is actually related to balancing of requirements for light, water and mechanical strength that will change with environmental conditions and tree ontogenetic stage.

4.3. Guying changes the pattern of biomass allocation in the tree stem: Use of DBH as a proxy to predict the root-soil mechanical properties might be risky

Preferential strengthening of the stem does not explain the apparent absence of guying effect on the mechanical properties of the root-soil plate that can be explained differently for thinned trees and for unthinned trees. Unthinned guyed trees exhibited very little growth so that it is difficult to detect any change in the mechanical properties compared to unthinned free trees considering the short treatment duration (4 years compared to 30 years of growth in same condition). In thinned and guyed trees, the root-soil mechanical properties are not significantly different from uTF trees while its stem biomass increased (Table 1) and that is why the relationship between the root-soil mechanical properties and its empirical predictor has changed. This effect is not the same for the stem resistance that scales with the DBH^3 and as you can see in Fig. 6. Both predictors do not react in the same way to guying. It indicates that using proxies to predict the root-soil plate performances (or DBH to predict the stem biomass) may be biased if allocation patterns are modified due to environmental stresses. In the next section, we will look at what happens in the structural roots to better understand the guying effect on the biomass allocation inside the tree.

4.4. Guying restricts the biomass allocation to mechanically stimulated tree parts while higher mechanical loading due to thinning is boosting the stem growth at the expense of structural roots reinforcement in line with the mechanical weak point location

Our experiment has a factorial design examining two treatments “thinning” and “guying”. It was aimed at studying how the thigmomorphogenesis controls and restores mechanical stability during the life of a tree, in natural conditions of disturbance from both resource availability and mechanical stimulation. In this paper, we focus on anchorage stability. As mechanical properties of the root-soil plate integrates 30 years of the growth in the same condition and only 4 years under different treatments, the effect of thinning and guying is not easy to track. We therefore looked not only on global properties (stem biomass, root-soil plate mechanical behaviour) but also at growth and the growth allocation between different tree compartments during the four years before and after the treatment to analyse changes in the biomass allocation. Fig. 5b shows that in thinned trees free to sway the biomass is preferentially allocated to the stem instead of roots, a pattern that is not observed in thinned and guyed trees. Furthermore, growth of both structural roots and the lower part of the stem is highly reduced in unthinned and guyed trees. In our dataset, the effect of thinning and guying was lower in the first year, which was the driest one, for both tree compartments with no delay between the root and the stem growth response (not shown). These results support the hypothesis of a

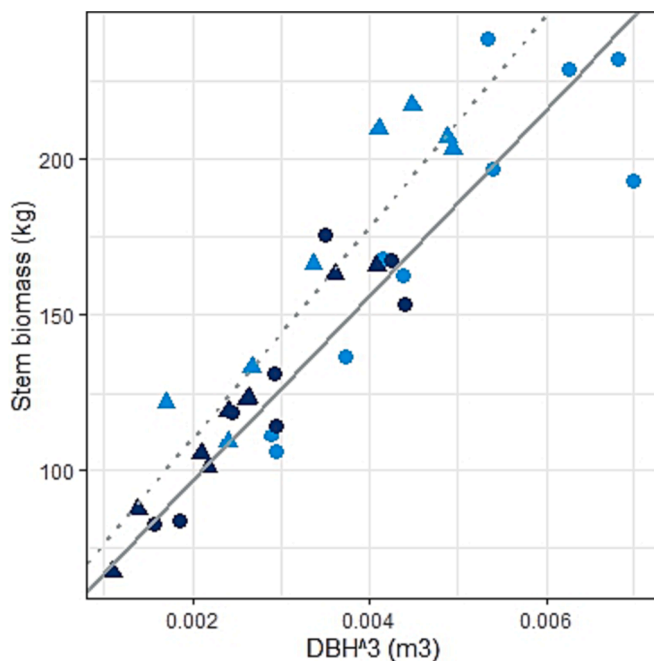


Fig. 6. Relationship between the stem biomass and the diameter at breast height elevated at power three for different treatments. Dark blue points represent unthinned trees. Light blue points represent thinned trees. Triangles stand for guyed trees and circles for trees free to sway. Solid grey line represents regression line for trees free to sway and dotted grey line represents regression line for guyed trees.

reinforcement of mechanically most stimulated and at risk points and suggest that further developments should investigate how the response is physiologically driven (how can growing cells be coordinated inside the whole tree to prioritize the weakest point) and how the priorities are enhanced in the case of poor light levels or water availability. Comparing life trajectories of mechanical risk for different tree species and compartments should be useful to develop a unified theory of the biomechanical control of growth allocation and its role in tree resistance to winds, using disturbance situations (thinning or other natural gap opening) to manipulate both growth and risk. Such a global view should provide help to develop further the current studies focused on a very limited range of species, ages and conditions. For instance, we might expect great differences between conifers and angiosperms.

5. Conclusion

In this paper, we examined the growth and mechanical properties of different tree compartments (stem and root/root-soil plate) in forty beech poles in a representative naturally regenerated managed forests in North Eastern France, with high stem density. We submitted trees to a factorial designed experiment with (i) thinning that stimulated growth and enhanced wind risk and mechanical stimuli, and (ii) guying that removed mechanical stimuli in stems and roots. After four years, we made field mechanical tests to quantify the root soil plate strength and stiffness, and we measured growth in different tree compartments. Our results showed a rather surprising decrease in the overturning moment for a given stem biomass in thinned trees while thigmomorphogenesis expects the opposite. A deeper analysis showed that the biomass was preferentially allocated to the stem at the expense of roots. We interpreted this shift in the biomass allocation as a response to lower mechanical risk predicted in roots compared to the stem. Providing a clear answer about how priorities of biomass allocation between the different compartments are controlled by mechanical risk and stimuli and/or by other factors as hydraulic functioning or soil constraints to root development is necessary to support innovative visions of growth allocation in respect to forest resistance and resilience, connecting ecological and silvicultural approaches to physiological knowledge on the response of growth processes from living cells to signalling (mechanical signals or others in interaction).

CRedit authorship contribution statement

Jana Dlouhá: Methodology, Formal analysis, Writing - original draft, Writing - review & editing. **Pauline Défossez:** Methodology. **François Ningre:** Writing - review & editing. **Joel Hans Dongmo Keumo Jiazet:** Data curation, Methodology. **Meriem Fournier:** Conceptualization, Methodology, Writing - review & editing. **Thierry Constant:** Conceptualization, Methodology, Funding acquisition, Writing - original draft, Writing - review & editing.

Declaration of Competing Interest

The authors declare that they have no known competing financial interests or personal relationships that could have appeared to influence the work reported in this paper.

Data availability

Data will be made available on request.

Acknowledgements

Authors sincerely thank all members of SilvaTech platform and Silviculture Pole of SILVA laboratory, INRAE Grand-Est for the technical help on the field and during the stem and root samples characterisation. This work was funded as part of a PhD project by supported by “Région

Grand Est” and the INRAE division ECODIV. This work was also supported by a grant overseen by the French National Research Agency (ANR) as part of the “Investissements d’Avenir” program (ANR-11-LABX-0002-01, Lab of Excellence ARBRE).

References

- Achim, A., Ruel, J.C., Gardiner, B.A., 2005a. Evaluating the effect of precommercial thinning on the resistance of balsam fir to windthrow through experimentation, modelling, and development of simple indices. *Can. J. For. Res.* 35, 1844–1853. <https://doi.org/10.1139/x05-130>.
- Achim, A., Ruel, J.C., Gardiner, B.A., Laflamme, G., Meunier, S., 2005b. Modelling the vulnerability of balsam fir forests to wind damage. *For. Ecol. Manage.* 204, 35–50. <https://doi.org/10.1016/j.foreco.2004.07.072>.
- Albrecht, A.T., Fortin, M., Kohnle, U., Ningre, F., 2015. Coupling a tree growth model with storm damage modeling – Conceptual approach and results of scenario simulations. *Environ Model Softw.* 69, 63–76. <https://doi.org/10.1016/j.envsoft.2015.03.004>.
- Albrecht, A., Hanewinkel, M., Bauhus, J., Kohnle, U., 2012. How does silviculture affect storm damage in forests of south-western Germany? Results from empirical modeling based on long-term observations. *Eur. J. For. Res.* 131, 229–247. <https://doi.org/10.1007/s10342-010-0432-x>.
- Bonnesoeur, V., Fournier, M., Bock, J., Badeau, V., Fortin, M., Colin, F., 2013. Improving statistical windthrow modeling of 2 *Fagus sylvatica* stand structures through mechanical analysis. *For. Ecol. Manage.* 289, 535–543. <https://doi.org/10.1016/j.foreco.2012.10.001>.
- Bonnesoeur, V., Constant, T., Moulia, B., Fournier, M., 2016. Forest trees filter chronic wind-signals to acclimate to high winds. *New Phytol.* 210, 850–860. <https://doi.org/10.1111/nph.13836>.
- Bréda, N., Granier, A., Aussenac, G., 1995. Effects of thinning on soil and tree water relations, transpiration and growth in an oak forest (*Quercus petraea* (Matt) Liebl). *Tree Physiol.* 15, 295–306. <https://doi.org/10.1093/treephys/15.5.295>.
- Brudi, E., Wassenaar, P., 2001. Trees and statics: nondestructive failure analysis. In: Thomas ES, K.D. (Ed.), *Tree Structure and Mechanics Conference Proceedings: How Trees Stand up and Fall down*. International Soc. of Arboriculture. pp. 53–69.
- Constant, T., Bonnesoeur, V., Chaumet, M., Ningre, F., Farré, E., Fournier, M., Moulia, B., 2018. Disentangling the effects of mechanical stimulations in the tree growth response after thinning: First results of an experiment carried out in a beech stand. In: *9th International Plant Biomechanics Conference*, August. Montreal, Canada, pp. 9–14.
- Coutts, M.P., 1986. Components of Tree Stability in Sitka Spruce on Peaty Gley Soil. *For. an Int. J. for. Res.* 59, 173–197. <https://doi.org/10.1093/forestry/59.2.173>.
- Coutts, M.P., Nielsen, C.C.N., Nicoll, B.C., 2000. The development of symmetry, rigidity and anchorage in the structural root system of conifers. In: Stokes, A. (Ed.), *The Supporting Roots of Trees and Woody Plants: Form, Function and Physiology*. Springer, Netherlands, Dordrecht, pp. 3–17. https://doi.org/10.1007/978-94-017-3469-1_1.
- Cremer, K.W., Borough, C.J., McKinnell, F.H., Carter, P.R., 1982. Effects of stoking and thinning on wind damage in plantations. *New Zeal. J. for. Sci.* 12, 244–268.
- Cucchi, V., Meredieu, C., Stokes, A., Berthier, S., Bert, D., Najjar, M., Denis, A., Lastennet, R., 2004. Root anchorage of inner and edge trees in stands of Maritime pine (*Pinus pinaster*Ait.) growing in different podzolic soil conditions. *Trees* 18, 460–466. <https://doi.org/10.1007/s00468-004-0330-2>.
- Défossez, P., Rajaonalison, F., Bosc, A., 2022. How wind acclimation impacts *Pinus pinaster* growth in comparison to resource availability. *Forestry* 95, 118–129. <https://doi.org/10.1093/forestry/cpab028>.
- Detter, A., Rust, S., Krišāns, O., 2023. Experimental Test of Non-Destructive Methods to Assess the Anchorage of Trees. *Forests* 14. <https://doi.org/10.3390/f14030533>.
- Dongmo Keumo Jiazet, J.H., 2022. *Acclimation of trees to increased wind loads following thinning in a Beech stand* (Doctoral dissertation). AgroParisTech.
- Dongmo Keumo Jiazet, J.H., Dlouha, J., Fournier, M., Moulia, B., Ningre, F., Constant, T., 2022. No matter how much space and light are available, radial growth distribution in *Fagus sylvatica* L. trees is under strong biomechanical control. *Ann. For. Sci.* 79. <https://doi.org/10.1186/s13595-022-01162-8>.
- Dupuy, L.X., Fourcaud, T., Lac, P., Stokes, A., 2007. A generic 3d finite element model of tree anchorage integrating soil mechanics and real root system architecture. *Am. J. Bot.* 94, 1506–1514. <https://doi.org/10.3732/ajb.94.9.1506>.
- Fox, J., Weisberg, S., 2019. *An R Companion to Applied Regression*, 3rd ed. Sage, Thousand Oaks (CA).
- Gardiner, B., Peltola, H., Kellomaki, S., 2000. Comparison of two models for predicting the critical wind speeds required to damage coniferous trees. *Ecol. Model.* 129, 1–23. [https://doi.org/10.1016/S0304-3800\(00\)00220-9](https://doi.org/10.1016/S0304-3800(00)00220-9).
- Gardiner, B., Byrne, K., Hale, S., Kamimura, K., Mitchell, S.J., Peltola, H., Ruel, J.-C., 2008. A review of mechanistic modelling of wind damage risk to forests. *Forestry* 81, 447–463. <https://doi.org/10.1093/forestry/cpn022>.
- Hale, S.E., Gardiner, B.A., Wellpott, A., Nicoll, B.C., Achim, A., 2012. Wind loading of trees: influence of tree size and competition. *Eur. J. For. Res.* 131, 203–217. <https://doi.org/10.1007/s10342-010-0448-2>.
- James, K., Hallam, C., Spencer, C., 2013. Tree stability in winds: Measurements of root plate tilt. *Biosyst. Eng.* 115, 324–331. <https://doi.org/10.1016/j.biosystemseng.2013.02.010>.
- Jonsson, M.J., Foetzki, A., Kalberer, M., Lundstroem, T., Ammann, W., Stoeckli, V., 2006. Root-soil rotation stiffness of Norway spruce (*Picea abies* (L.) Karst) growing on

- subalpine forested slopes. *Plant Soil* 285, 267–277. <https://doi.org/10.1007/s11104-006-9013-7>.
- Kamimura, K., Gardiner, B.A., Koga, S., 2017. Observations and predictions of wind damage to *Larix kaempferi* trees following thinning at an early growth stage. *Forestry* 90, 530–540. <https://doi.org/10.1093/forestry/cpx006>.
- Kneeshaw, D., Williams, H., Nikinmaa, E., Messier, C., 2002. Patterns of above- and below-ground response of understory conifer release 6 years after partial cutting. *Can. J. For. Res.* 32, 255–265. <https://doi.org/10.1139/X01-190>.
- López, B.C., Sabate, S., Gracia, C.A., 2003. Thinning effects on carbon allocation to fine roots in a *Quercus ilex* forest. *Tree Physiol.* 23, 1217–1224. <https://doi.org/10.1093/treephys/23.17.1217>.
- Lundstrom, T., Jonsson, M.J., Kalberer, M., 2007. The root-soil system of Norway spruce subjected to turning moment: resistance as a function of rotation. *Plant Soil* 300, 35–49. <https://doi.org/10.1007/s11104-007-9386-2>.
- Mitchell, S.J., 2000. Stem growth responses in Douglas-fir and Sitka spruce following thinning: implications for assessing wind-firmness. *For. Ecol. Manag.* 135, 105–114. [https://doi.org/10.1016/S0378-1127\(00\)00302-9](https://doi.org/10.1016/S0378-1127(00)00302-9).
- Mouliat, B., Coutand, C., Julien, J.-L., 2015. Mechanosensitive control of plant growth: bearing the load, sensing, transducing, and responding. *Front. Plant Sci.* 6, 52.
- Nicoll, B., Achim, A., Crossley, A., Gardiner, B., Mochan, S., 2009. The effects of spacing on root anchorage and tree stability. *Scottish for.* 63, 32–36.
- Nicoll, B.C., Connolly, T., Gardiner, B.A., 2019. Changes in Spruce Growth and Biomass Allocation Following Thinning and Guying Treatments. *Forests* 10, 253.
- Nicoll, B.C., Dunn, A.J., 2000. The effects of wind speed and direction on radial growth of structural roots. In: Stokes, A. (Ed.), *The Supporting Roots of Trees and Woody Plants: Form, Function and Physiology*. Springer, Netherlands, Dordrecht, pp. 219–225. https://doi.org/10.1007/978-94-017-3469-1_21.
- Nicoll, B.C., Gardiner, B.A., Rayner, B., Peace, A.J., 2006. Anchorage of coniferous trees in relation to species, soil type, and rooting depth. *Can. J. for. Res. Can. Rech. for.* 36, 1871–1883. <https://doi.org/10.1139/X06-072>.
- Nicoll, B.C., Gardiner, B.A., Peace, A.J., 2008. Improvements in anchorage provided by the acclimation of forest trees to wind stress. *Forestry* 81, 389–398. <https://doi.org/10.1093/forestry/cpn021>.
- Nicoll, B.C., Ray, D., 1996. Adaptive growth of tree root systems in response to wind action and site conditions. *Tree Physiol.* 16, 891–898.
- Olivar, J., Bogino, S., Rathgeber, C., Bonnesoeur, V., Bravo, F., 2014. Thinning has a positive effect on growth dynamics and growth-climate relationships in Aleppo pine (*Pinus halepensis*) trees of different crown classes. *Ann. For. Sci.* 71, 395–404. <https://doi.org/10.1007/s13595-013-0348-y>.
- Pang, Y., Tian, J., Yang, H., Zhang, K., Wang, D., 2022. Responses of Fine Roots at Different Soil Depths to Different Thinning Intensities in a Secondary Forest in the Qinling Mountains, China. *Biol.-Basel* 11. <https://doi.org/10.3390/biology11030351>.
- Peltola, H.M., 2006. Mechanical stability of trees under static loads. *Am. J. Bot.* 93, 1501–1511. <https://doi.org/10.3732/ajb.93.10.1501>.
- Peltola, H., Kellomäki, S., Hassinen, A., Granander, M., 2000. Mechanical stability of Scots pine, Norway spruce and birch: an analysis of tree-pulling experiments in Finland. *For. Ecol. Manag.* 135, 143–153. [https://doi.org/10.1016/S0378-1127\(00\)00306-6](https://doi.org/10.1016/S0378-1127(00)00306-6).
- R Core Team, 2020. R: A Language and Environment for Statistical Computing. <https://doi.org/10.1038/sj.hdy.6800737>.
- Rudnicki, M., Meyer, T.H., Lieffers, V.J., Silins, U., Webb, V.A., 2008. The periodic motion of lodgepole pine trees as affected by collisions with neighbors. *Trees* 22, 475–482. <https://doi.org/10.1007/s00468-007-0207-2>.
- Ruel, J.C., Larouche, C., Achim, A., 2003. Changes in root morphology after precommercial thinning in balsam fir stands. *Can. J. for. Res. Can. Rech. for.* 33, 2452–2459. <https://doi.org/10.1139/X03-178>.
- Schneider, C.A., Rasband, W.S., Eliceiri, K.W., 2012. NIH Image to ImageJ: 25 years of image analysis. *Nat. Methods* 9, 671–675. <https://doi.org/10.1038/nmeth.2089>.
- Stokes, A., 2000. *The supporting roots of trees and woody plants: form, function and physiology*. Kluwer Academic Publishers, Dordrecht, Netherlands.
- Telewski, F.W., 2006. A unified hypothesis of mechanoperception in plants. *Am. J. Bot.* 93, 1466–1476. <https://doi.org/10.3732/ajb.93.10.1466>.
- Urban, S.T., Lieffers, V.J., Macdonald, S.E., 1994. Release in radial growth in the trunk and structural roots of white spruce as measured by dendrochronology. *Can. J. for. Res. Can. Rech. for.* 24, 1550–1556. <https://doi.org/10.1139/x94-202>.
- Valinger, E., Fridman, J., 2011. Factors affecting the probability of windthrow at stand level as a result of Gudrun winter storm in southern Sweden. *For. Ecol. Manag.* 262, 398–403. <https://doi.org/10.1016/j.foreco.2011.04.004>.
- Vincent, M., Krause, C., Zhang, S.Y., 2009. Radial growth response of black spruce roots and stems to commercial thinning in the boreal forest. *Forestry* 82, 557–571. <https://doi.org/10.1093/forestry/cpp025>.
- Wallentin, C., Nilsson, U., 2014. Storm and snow damage in a Norway spruce thinning experiment in southern Sweden. *Forestry* 87, 229–238. <https://doi.org/10.1093/forestry/cpt046>.
- Webb, V.A., Rudnicki, M., Muppa, S.K., 2013. Analysis of tree sway and crown collisions for managed *Pinus resinosa* in southern Maine. *For. Ecol. Manag.* 302, 193–199. <https://doi.org/10.1016/j.foreco.2013.02.033>.
- Yang, M., Defossez, P., Danjon, F., Fourcaud, T., 2018. Analyzing key factors of roots and soil contributing to tree anchorage of *Pinus* species. *Trees-Struct. Funct.* 32, 703–712. <https://doi.org/10.1007/s00468-018-1665-4>.
- Yang, M., Defossez, P., Dupont, S., 2020. A root-to-foilage tree dynamic model for gusty winds during windstorm conditions. *Agric. For. Meteorol.* 287. <https://doi.org/10.1016/j.agrformet.2020.107949>.